JCTC Journal of Chemical Theory and Computation

Article

pubs.acs.org/JCTC

An ab Initio Benchmark and DFT Validation Study on Gold(I)-Catalyzed Hydroamination of Alkynes

Gianluca Ciancaleoni,[†] Sergio Rampino,[†] Daniele Zuccaccia,[‡] Francesco Tarantelli,[§] Paola Belanzoni,*[,§] and Leonardo Belpassi*[,†]

[†]Istituto di Scienze e Tecnologie Molecolari del CNR c/o Dipartimento di Chimica, Biologia e Biotecnologie, Università di Perugia, 06123, Italy

[‡]Dipartimento di Chimica, Fisica e Ambiente, Università di Udine, Via Cotonificio 108, I-33100 Udine, Italy

[§]Dipartimento di Chimica, Biologia e Biotecnologie, Università di Perugia, 06123, Italy

Supporting Information

ABSTRACT: High level ab initio calculations have been carried out on an archetypal gold(I)-catalyzed reaction: hydroamination of ethyne. We studied up to 12 structures of possible gold(I)-coordinated species modeling different intermediates potentially present in a catalytic cycle for the addition of a protic nucleophile to an alkyne. The benchmark is used to evaluate the performances of some popular density functionals for describing geometries and relative energies of stationary points along the reaction profile. Most functionals (including hybrid or meta-hybrid) give accurate structures but large nonsystematic errors (4−12 kcal/mol) along the reaction energy profile. The double hybrid functional B2PLYP outperforms all considered functionals and compares very nicely with our reference ab initio benchmark energies. Moreover, we present an assessment of the accuracy of commonly used approaches to include relativistic effects, such as relativistic effective potentials and a scalar ZORA Hamiltonian, by a comparison with the results obtained using a relativistic all-electron four-component Dirac−Kohn−Sham method. The contribution of nonscalar relativistic effects in gold(I)-catalyzed reactions, as we investigated here, is expected to be on the order of 1 kcal/mol.

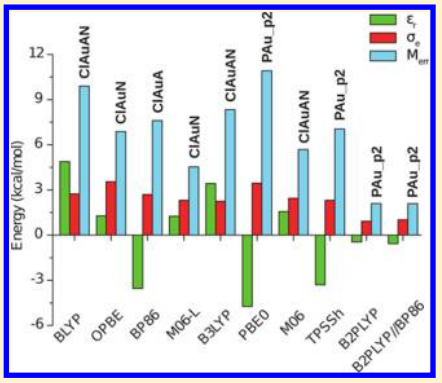

INTRODUCTION

Over the past decade, Density Functional Theory (DFT)[1−3] has been the framework of choice for the study of complex reaction mechanisms and for characterizing transition states and intermediates in chemical transformations. In these studies, an evaluation of the performance of different exchange-correlation density functionals (DFs) on series of realistic chemical tasks is normally a necessary step prior to their use for the investigation of new problems. Although several sets were developed in recent years to test DFs in the treatment of the main-group chemistry, less extensive benchmarks exist in the field of transition-metal chemistry and bond activation by transition-metal catalysts.[4,5] An area of great interest in this context is that of gold(I) complexes, which have emerged in the past few years as excellent catalysts in numerous homogeneous organic transformations involving unsaturated hydrocarbons (UHC),[6−10] due to the unique ability of gold to coordinate and activate such species toward nucleophilic attack. In fact, different types of L-Au(I) complexes of high catalytic activity can be obtained under different conditions, and it is known that the ligand L plays a major role in tuning the reactivity and selectivity of the process in homogeneous gold(I)-mediated reactions.

A prototypical catalytic cycle for the addition of a protic nucleophile (NuH) to an alkyne is shown in Figure 1, but many reactions involving gold-promoted activation of unsaturated compounds are not as simple as they appear, because numerous short-lived intermediates and ramifications in the reaction paths

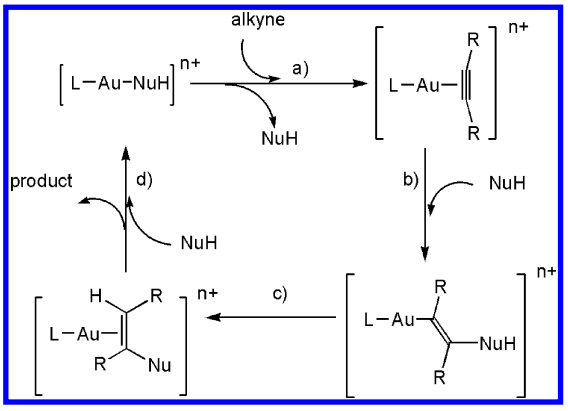

Figure 1. Key steps involved in a catalytic cycle for the addition of a protic nucleophile (NuH) to an alkyne. (a) Substrate substitution, (b) nucleophilic attack, (c) protodeauration, (d) product release and catalyst regeneration.

Received: November 12, 2013
Published: February 5, 2014

may be involved. This makes both the experimental and theoretical study of the mechanisms a difficult task. Among others, the linear biscoordinated $[LAu(UHC)]^{+n}$ (n = 0, 1) complexes are hypothesized to be key intermediates in catalyzed transformations. Intermediates of this type have been recently isolated and characterized.[11−18] In the first step, UHC coordination to Au often involves substitution of a coordinated molecule,[19−22] and the latter can be the nucleophilic species itself,[23] the solvent, or the counterion (anion).[24] When the UHC replaces a coordinated protic nucleophile—the case depicted in Figure 1—either a dissociative or an associative pathway can be taken, where bis- and tricoordinated Au(I) species are involved, respectively. In the second step, the nucleophilic attack toward the linear biscoordinated $[LAu(UHC)]^{+n}$ complex can occur through an intra- or intermolecular pathway (inner-sphere or outer-sphere mechanism), which again may involve different Au(I)-coordinated species. In the third step, the protodeauration[25] takes place, where a proton is transferred to the carbon that is σ-coordinated to the gold atom, and finally, in the last step, the product is released and the catalyst is regenerated. Protodeauration is unfavored in the gas phase,[26] but it can be greatly facilitated by the proton shuttle provided by the solvent,[24,26] the counterion,[27] or the nucleophile species itself.[27] The relative importance of the nucleophilic addition and protodeauration as the rate-determining step depends on many details, such as the nature of the ancillary ligand, the strength of the nucleophile, the presence of cocatalysts, and the solvent. To understand and categorize all these aspects, further theoretical study of the mechanism of alkyne activation providing the reason why Au(I) complexes have a catalytic effect and what factors influence their catalytic activity is highly desirable. However, as mentioned earlier, prior to such intensive and challenging investigations, a validation of the DFT framework to be used, against an ab initio benchmark, is of crucial importance. To meaningfully accomplish this, in a scenario where numerous intermediates can be found along the reaction profile and the individual reaction steps are very often characterized by very small energy barriers, even in the simplified mechanism depicted in Figure 1, we reasoned that the density functional validation should focus on the overall reaction mechanism, permitting the differentiation between competitive paths, characterization of intermediates, or provision of a step-by-step description of the structure and energy changes along the reaction profile. We decided to study a number of possible Au(I)-coordinated species modeling different intermediates potentially present in a catalytic cycle for the addition of a protic nucleophile to an alkyne. The aim is to find suitable exchange-correlation functionals which allow us to gain a reasonably balanced description of the different species and lead to a better understanding of Au(I) catalysis and an improved predictive capability of reactivity.

Some theoretical groups have recently been studying the chemistry of gold, both in its fundamental aspects, such as the influence of relativistic effects on the peculiar properties of the gold atom,[28,29] and with regard to the mechanism of gold-catalyzed reactions.[30]

Most of the computational studies[27,31,32] on realistic gold-catalyzed reaction mechanisms are based on DFT methods, usually employing a standard hybrid functional, i.e., the B3LYP functional, a double-ζ polarized 6-31G(d) (or 6-31G*) basis set and a scalar relativistic effective core potential (RECP) for the heavy atom. A single point refinement employing a larger basis set (usually, a triple-ζ basis set with polarization and diffuse functions added) is often considered good enough, sometimes also using a different functional that showed a good performance with transition metal complexes.

As far as we know, there are only few recent papers on gold complexes reporting benchmark studies devoted to assessing the accuracy of different approximations to the DFT exchange-correlation functional. Two of them concern the simple Au-UHC η^2 interaction.[33,34] Chen et al.[33] benchmarked many density functionals for a variety of Au(I)/Au(III) complexes with UHC substrates (ethene, ethyne, and allene). Their findings are that the best performing DFs are double-hybrids (B2GPPLYP and B2PLYP) for both the geometry and bond dissociation energy, and a dispersion correction (DFT-D3) does not uniformly improve the results of all functionals. Nava and co-workers[34] investigated small Au(I) complexes interacting with ethyne and ethene. Their work showed that different multireference methods including MRCI converge nicely to the monodeterminantal reference coupled cluster approach (CCSD(T)). Among the tested DFs, a GGA as BP86 and a meta-GGA as TPSS reproduce their reference CCSD(T) results, M06 provides an acceptable performance, while a hybrid DF as B3LYP shows the largest errors. The work showed that the Au(I)-UHC interaction depends strongly on the substituents in the unsaturated substrate that result in a significant dis-symmetry in UHC coordination.

Recently, Pašteka et al.[35] published CCSD(T) interaction energies and bonding analysis for complexes of Cu, Ag, and Au with a variety of lone-pair ligands, among them H_2O, NH_3, and PH_3, underlining that both electron correlation and relativistic effects are crucial in the bonding of all complexes. The strongest interactions are computed for PX_3 (X = H, F, Cl) ligands followed by SX_2 and NX_3 and OX_2 ligands. In particular, the exceptional stability of gold complexes has been attributed to large relativistic enhancement of the electron affinity of Au. Benchmark CCSD(T) interaction energies are used to test different DFs, with the hybrid PBE0 functional providing the correct pattern. A paper by Chen et al. deals with the late transition-metal-catalyzed reactions with Au, Pt, and Ir, and it is devoted to assessing the accuracy of a new scheme of Local Coupled Cluster methods in computing activation energies.[36] They calibrated the performance of several DFs, and the main conclusion was that the best functional is the double-hybrid B2GPPLYP, with other well-performing functionals including M06-2X, BMK, PBE0, and wB97X, but also that different types of reactions may require different types of optimal DFT methods. Only one paper, by Faza and co-workers, analyzes different steps of a reaction mechanism.[37] In their work, the considered system is the "golden carousel" experimentally and theoretically studied by Nolan and co-workers for the Au-catalyzed 1,2- and 1,3-acyl migration in propargylic esters.[38] They simplified the organic substrate to a propargylic acetate and the catalyst to $AuPH_3^+$ and benchmarked 32 DFs against high-level computational data obtained at the CCSD/def2-TZVPP level of theory as a reference. This study reveals that accurate results for intermediates are only given by the last generation of DFs, among them M06 and B2PLYP generally outperforming the rest, and that a careful selection of basis set and electron core potentials can be critical to achieving high accuracy. The reference geometries were obtained at the CCSD level with a relatively small basis set (def2-SVP). The use of a such reference data for benchmarking DFs has been recently doubted by Nava et al.[34]

All of the theoretical studies reported in the literature include relativistic effects on a scalar level using either relativistic effective potential (RECP) or all-electron approaches based on

Douglass−Kroll−Hess transformation or zero-order relativistic approximation (ZORA). The knowledge of nonscalar relativistic effects, like spin−orbit coupling, on the reaction path of heavy transition metal is still limited and largely unexplored in the context of gold(I)-based reactions. Recently, Chen et al.[39] showed that nonscalar relativistic effects play a role in the Pt-catalyzed C−H activation increasing the barrier of the process by about 1 kcal/mol. The authors showed that the effect is on par with the solvent effect corrections or thermal free energy corrections. We note that spin−orbit coupling is found to be essential for a complete understanding of the reactions involving heavy transition metal open-shell systems.[40,41]

In the present work, we investigate the mechanism of a specific prototype of the reaction given in Figure 1, the nucleophilic attack of ammonia on ethyne catalyzed by either a neutral, AuCl, or a cationic, $[PH_3Au]^+$, gold(I) complex. This represents the simple prototype of the reaction of hydroamination of alkynes mediated by gold(I) catalysts, which has attracted great attention from both the experimental and theoretical sides.[23,24,27,31,42−44] The purpose of our study is two-fold. In the first place, we wish to obtain a reliable benchmark for the gold(I)-coordinated species (both geometries and complexation energies), which could be involved in the proposed mechanism for the Au(I)-catalyzed hydroamination of alkynes. This is done by exploring plausible Au(I) coordination geometries with a hierarchical series of ab initio methods including second-order Møller−Plesset perturbation theory (MP2), Density Fitting Local Coupled Cluster theory with single and double excitations (DF-LCCSD) and with triple excitations treated perturbatively [DF-LCCSD(T)], and, for reliable benchmark energies, canonical Coupled Cluster theory with single and double excitations and with triple excitations treated perturbatively [CCSD(T)], in combination with a hierarchical series of Gaussian-type basis sets of increasing flexibility and polarization. We focus on the transition state (TS) for the nucleophilic attack step, possible intermediate geometries along the reaction path, and the energies of the individual species relative to the free reactants, that is, LAu + NH_3 + C_2H_2, in the gas phase. The second purpose of our work is to evaluate the performance of a number of popular DFs, covering GGA, meta-GGA, hybrid, double-hybrid, and meta-hybrid types, for describing the substrate substitution (i.e., NH_3 substitution by C_2H_2 at Au center) and the nucleophilic attack of NH_3 toward C_2H_2 coordinated to Au, using our ab initio benchmark as a reference point. A general concern associated with the application of DFT to the investigation of transition metal catalyzed reactions is the convergence of the results with basis set extension (size, dispersion, and diffusion functions effects) for both geometries and energies of the different metal-coordinated species. It is known that, due to the variable occupation of the valence d orbitals, the treatment of transition metal compounds requires special care in the basis set choice even at the DFT level.[45,46] Then, our survey of a few popular density functionals serves to validate one or more of these DFT approaches as a computationally more efficient alternative to high-level ab initio theory in future investigations in the field of computational gold catalysis and in particular for the hydroammination reaction involving realistic species. Finally, a detailed analysis of available tools to include relativistic effects, on both the scalar and nonscalar level, has also been carried out, comparing the data obtained using the realtivistic effective potential (RECP), all-electron approximated Hamiltonian as ZORA, and a full relativistic approach based on the Dirac−Kohn−Sham methodology.

METHOD AND COMPUTATIONAL DETAILS

All ab initio calculations were carried out with the parallel version of MOLPRO2010.1[47,48] program package, whereas for DFT calculations we used the Gaussian 09 revision A[49] and Turbomole 6.3 programs.[50] For reliable benchmark geometries, the structures of the considered species were optimized ab initio using the Local Coupled Cluster method with single and double excitations and a perturbative treatment of triple excitation [LCCSD(T)] as implemented in MOLPRO in combination with the Ahlrichs basis set of Gaussian-type orbitals (GTOs) of triple-ζ quality TZVPP (or def2-TZVPP using the same notation as in Turbomole 6.3). To reduce the computational cost, density fitting approximations were employed in the LCCSD and LCCSD(T) calculations, using the corresponding auxiliary basis sets.[51−53] These methods are referred to as DF-LCCSD and DF-LCCSD(T). Scalar relativistic effects have been introduced by using effective core potential (RECP) on gold atoms for the description of the 60 innermost electrons with the associated basis sets.[54] The comparison with the results obtained for interaction energies in some related systems, using different Hamiltonians, as for instance the all-electron Douglas−Kroll−Hess approach, shows an accuracy of RECP higher than 1 kcal/mol.[33,55] In this work, the Au 5s5p core−valence correlation effects were not considered for all the ab initio calculations. These effects are not negligible (about 1−2 kcal/mol) in absolute value,[33] but they are expected to be quite systematic along a reaction path. These effects are on the same order of magnitude (but opposed in sign) as the error introduced by the use of RECP,[33] and in Au-catalyzed reaction barrier calculations these core−valence correlation effects are found to be small and negligible.[36] The accuracy of the reference geometries was investigated for the smaller systems with the canonical coupled cluster method (CCSD(T)) employing a detailed analysis of convergence with respect to the increase of basis set size (def2-SVP, def2-TZVPP, and def2-QZVPP[54]). For completeness, also MP2 and DF-LCCSD geometry optimizations, using the same def2-TZVPP basis set, and DF-LCCSD(T) geometry optimizations, using a smaller double-ζ quality basis set def2-SVP, have been performed. The default distance criteria in the MOLPRO program for pair classification in local correlation approaches were used (R_{close} = 1 au, R_{weak} = 3 au). Vibrational analyses were carried out in order to verify that the optimized geometries were characterized by one (transition states) or no (equilibrium structures) imaginary frequencies. The optimized geometries at the DF-LCCSD(T)/def2-TZVPP level of theory were taken as references and were used for a single-point calculation using CCSD(T)[56−59] in combination with a GTO quadruple-ζ quality Ahlrichs basis set, def2-QZVPP, in order to obtain our reference energies.

A variety of popular DFs, namely BLYP, OPBE, BP86, M06-L, B3LYP, PBE0, M06, TPSSh, and B2PLYP in conjunction with different basis sets, have been tested, for both geometry optimization and energy calculations of the considered species. Unless otherwise indicated, the computations were carried out using def2-TZVP GTOs (Gaussian 09 and Turbomole 6.3). We used for each calculation the same specified basis set quality for all atoms. It should be noted that a balanced basis set should be employed; i.e., a large basis on the metal with a more modest basis on the other atoms, or vice versa, would give inaccurate results.[46] In order to compare the energies of the individual species calculated by different computational methods, the sum of the energies of all the isolated fragments was taken as a

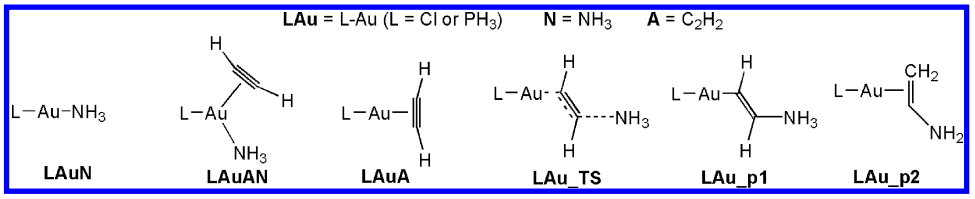

Figure 2. Structures of the stationary points along the reaction path for the $[LAu(I)]^{+n}$-catalyzed hydroamination of ethyne by ammonia (L = Cl, PH_3; n = 0, 1) and nomenclature.

reference (if not indicated differently) and set as the zero-point energy for all the combinations of functional/basis sets used. All calculations were performed for the closed shell singlet state.

The all-electron calculations using the scalar zero-order regular approximation (ZORA)[60] have been done in combination with all-electron QZVPP Slater-type orbitals (STOs) using the ADF 2010.01 code (version 2010)[61−63] in combination with a really fine integration parameter (with a numerical integration parameter set to 10). The full relativistic Dirac−Kohn−Sham (DKS) calculations used as reference to estimate the effect of nonscalar relativistic effects have been carried out with the DKS module of the four component code BERTHA.[64−67] The code uses the proper relativistic G-spinor basis set.[66] In this case, the large component basis set has been obtained by decontracting the def2-QZVPP basis set used on hydrogen, carbon, nitrogen, and phosphorus. The limit quadruple-ζ quality basis sets (34s30p19d12f3g1h) by Dyall were used for gold atoms.[68,69] The corresponding small-component basis was generated using the restricted kinetic balance relation.[70] For further details, we refer the reader to ref 64.

RESULTS AND DISCUSSION

Selection of the Reference Complexes. First, we examine different possible gold(I)-coordinated intermediates involved in the simple mechanism illustrated in Figure 1. As we mentioned, we shall here consider the simplified reaction of hydroamination in which NuH is the ammonia molecule, the alkyne is the ethyne substrate prototype, and the catalysts are the neutral ClAu or charged PH_3Au^+. Within this model, we will be able to compute both reference geometries and energies at the highest level of ab initio methods. The set of investigated selected species is summarized in Figure 2. The linear biscoordinated complexes, here $[(PH_3)Au(C_2H_2)]^+$ and $[ClAu(C_2H_2)]$, are usually hypothesized to be key intermediate species in these catalyzed transformations. However, different plausible gold(I)-coordinated species are conceivable. At least two different coordinating species are clearly available, that is, ammonia and ethyne, and thus different species can be formed, in principle: LAuN compounds, that is, $[ClAu(NH_3)]$ (hereafter denoted as ClAuN) or $[(PH_3)Au(NH_3)]^+$ (PAuN); LAuA compounds, that is, $[ClAu(C_2H_2)]$ (ClAuA) or $[(PH_3)Au(C_2H_2)]^+$ (PAuA); and tricoordinated species LAuAN, which stands for $[ClAu(C_2H_2)(NH_3)]$ (ClAuAN) or $[(PH_3)Au(C_2H_2)(NH_3)]^+$ (PAuAN). Tricoordinated species are rarely considered to be involved in the mechanism. However, since the first step of the reaction mechanism in Figure 1 is the substitution of a nucleophile by an alkyne substrate, either a dissociative or an associative pathway can be taken. Although gold is known to form mainly linear, biscoordinated complexes, some tricoordinated species have been isolated even with hindered ligands,[71−73] and many experimental studies indicate that ligand exchange proceeds through an associative mechanism,[74−76] which involves a tricoordinated species as the intermediate or transition state.

Regarding the transition state of the nucleophilic attack, many authors agree, on the basis of experimental[23,77,78] and theoretical[27] data, that the nucleophile species attacks the unsaturated C−C bond in an *anti* manner with respect to the gold atom (outer-sphere mechanism). We denote these transition states species as ClAu_TS and PAu_TS and the intermediate species resulting from the nucleophilic attack as ClAu_p1 and PAu_p1. Since for a realistic description of the protodeauration process a proton shuttle is required and the Au coordination does not substantially change, we will not consider the transition state structures for this step in our gas phase calculations. The intermediate species generated from this step, where the gold atom has been formally substituted by a proton coming from the coordinated NH_3, are denoted as ClAu_p2 and PAu_p2. Finally, the product 1-amino-ethene can be directly released or it can undergo a rearrangement around the gold.[27]

Benchmark Geometries from ab Initio Calculations. The fully optimized structures computed at the DF-LCCSD(T) level of theory using the def2-TZVPP basis set, without any symmetry constraints, are displayed in Figure 3. The figure shows the computed values of the main geometrical parameters.

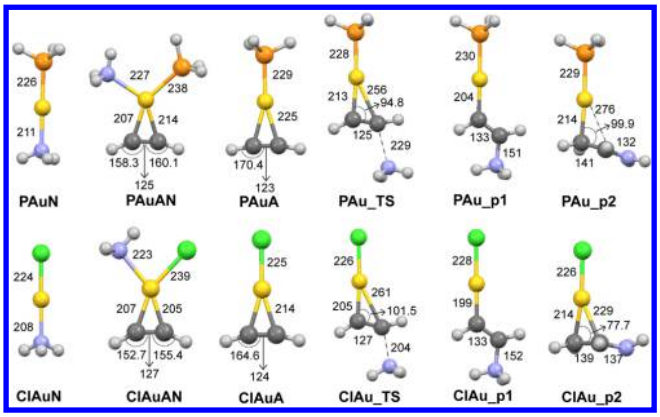

Figure 3. Reference structures optimized at the DF-LCCSD(T)/def2-TZVPP level of theory. Distances are in picometers, angles in degrees.

The imaginary frequency in the transition state associated with the nucleophilic attack step has also been computed as 452 and 267 cm^{-1}, for ClAu_TS and PAu_TS, respectively. In the case of the smaller systems, PAuA, ClAuA, PAuN, and ClAuN, a detailed basis set convergence study has been carried out. We can summarize the results concluding that, within the DF-LCCSD(T) method, the def2-TZVPP basis set reproduces in practice the same geometries obtained using the limit def2-QZVPP basis set. In all cases, we found a maximum deviation of 1 pm. Our benchmark geometries obtained for PAuA and ClAuA can be directly compared with those obtained recently by Nava et al.[34] using the canonical CCSD(T) method and the def2-QZVPP basis set. Analogously, we find absolute deviations within 1 pm. These results make us confident in the reliability of our reference

dx.doi.org/10.1021/ct400980w | J. Chem. Theory Comput. 2014, 10, 1021−1034

Table 1. Mean Error (ε_r), Standard Deviation (σ_r), and Maximum Absolute Error (M_r) over the Complete Set of Au−Cl, Au−P, Au−C, and C−C Bond Lengths Obtained with Different ab Initio Methods (Reference: DF-LCCSD(T)/def2-TZVPP)[a]

	MP2			DF-LCCSD			DF-LCCSD(T)/def2-SVP		
	ε_r	σ_r	M_r	ε_r	σ_r	M_r	ε_r	σ_r	M_r
Au−Cl	−2.5	0.4	3.3 AuCl	−0.4	0.1	0.5 ClAu_p2	3.1	0.6	3.7 ClAu_p2
Au−P	−4.0	0.5	4.9 PAuAN	0.0	0.1	0.4 PAu	4.2	0.7	5.2 PAuAN
Au−C	−4.8	2.9	11.0 PAu_TS	−0.6	0.4	1.8 ClAu_TS	1.2	1.5	4.1 PAuA
C−C	0.0	0.7	1.2 ClAuAN	−0.5	0.2	0.7 ClAu_p2	0.9	0.2	1.3 PAu_p2

[a]Distances are in pm. The species corresponding to M_r are also indicated.

DF-LCCSD(T)/def2-TZVPP approach, which performs at the same level as the CCSD(T)/def2-QZVPP method for geometry calculations, at a significantly lower computational cost.

It is interesting to compare the two series of geometries for the cationic $[(PH_3)Au]^+$ and neutral [ClAu] complexes. Significant differences are found, especially for the PAuAN/ClAuAN and PAu_p2/ClAu_p2 pairs of structures. In the ClAu structures, the unsaturated C−C coordination to Au is nearly symmetric, with similar Au−C1 and Au−C2 bond lengths of 207 and 205 pm in ClAuAN and 214 and 229 pm in ClAu_p2. In the corresponding PH_3Au^+ structures, C−C coordination to Au is more "asymmetric," with Au−C1 and Au−C2 bond distances of 207 and 214 pm in PAuAN and 214 and 276 pm in PAu_p2. This nonsymmetric coordination and the strong distortion of PAu_p2, for which its C2, directly bound to the $[(PH_3)Au]^+$ moiety, appears to shift an sp^2 to an sp^3 hybridization (also confirmed by the short C−N distance in PAu_p2, which assumes a partial double bond character), suggest a remarkable preference of PH_3Au^+ to coordinate carbon in a σ-type fashion rather than in an η^2 coordination.

The PAuA/ClAuA and PAu_p1/ClAu_p1 pairs of structures are very similar, except that the Au−C1 and Au−C2 distances are longer for the phosphine systems. Notably, both transition state geometries show a strong asymmetry in ethyne coordination and a high degree of distortion, although less pronounced in PAu_TS than what we found in ClAu_TS. This last structure is closer to the product ClAu_p1 than what one finds in the corresponding phosphine systems (PAu_TS, PAu_p1). One may surmise such structural features to be reflected in the reaction energy profile, so that AuCl (PAu) is characterized by a late (early) transition state. We shall return to this issue later on.

The differences in the structures summarized above confirm the important ligand effect and the significant differences in the electronic properties of the two metal fragments.[16,79] This is also indicated by the differences in the CCH bending of coordinated ethyne in both biscoordinated and tricoordinated species (LAuA, LAuAN). The CCH bending of ethyne coordinated to a metal fragment can give detailed information on the nature of the bond and in particular on the metal-to-ligand π-backdonation.[80] The coordinated ethyne presents, in ClAuA and ClAuAN, a systematic, larger deviation from linearity (about 6°) than in the respective compounds with phosphine. Moreover, the tricoordinated species (PAuAN/ClAuAN) present a larger deviation (about 10°) than biscoordinated species. All these findings are in line with the fact that the π-backdonation from the LAu metal unit to ethyne is larger for L = Cl than for L = PH_3 and increases on going from a biscoordinated to a tricoordinated species.[80] The calculated tricoordinated PAuAN and ClAuAN structures resemble the 1,3,5-triazapentadienyl gold complex by Dias and co-workers, where the alkyne bending was also very pronounced.[81]

The geometries of all species have been also optimized at the MP2/def2-TZVPP and DF-LCCSD/def2-TZVPP levels. The use of reduced basis (def2-SVP) in DF-LCCSD(T) has also been tested. The comparison with the reference structures has been made by selecting important bond lengths, namely, Au−Cl, Au−P, Au−C, and C−C, to account for deviation in different types of bonding interactions, and by carrying out a statistical analysis. The statistical results for the complete set of structures are presented in Table 1 in condensed form, including the mean signed error (ε_r), which accounts for the accuracy of the level of calculation; the standard deviation from the bond length reference values (σ_r), which is a measure of its precision; and the maximum absolute error (M_r), which is useful to understand which species is the most difficult one to reproduce. The latter is also indicated in the table. Inspection of σ_r is an important tool to reveal the presence of systematic errors.

The results show that MP2 gives unsatisfactory predictions of the Au−Cl, Au−P, and Au−C bond lengths, underestimating reference data. The error is not systematic, in particular for the prediction of the Au−C distance, which presents a high value of σ_r with an M_r of 11 pm. DF-LCCSD, with only single and double excitations, gives very good results on the geometries. In this case, ε_r is smaller than 1 pm, and M_r is reduced to 1.8 pm. This agreement indicates that the inclusion of perturbative triple excitations is not crucial here. By contrast, the use of a sufficiently flexible basis set is mandatory to achieve high accuracy. Indeed, the data obtained at the DF-LCCSD(T) level using the smaller def2-SVP basis present large deviations. At least a def2-TZVPP basis set has to be used to achieve accurate reference structures. On the basis of these findings and on the fact that DF-LCCSD(T)/def2-TZVPP is the highest-level treatment we used for our systems, we chose the geometries optimized at this level of theory to compute the ab initio benchmark energies presented in the next section.

Benchmark Energies from ab Initio Calculations. As mentioned above, the stationary points considered in Figure 3 identify the basic chemical transformations (typical bond-forming and breaking) that may occur in the gold-catalyzed hydroamination of an alkyne substrate (Figure 1). Their relative energy is expected to be highly sensitive to the level of theory used. Here, we report a systematic investigation of the extent to which the complexation energy values are converged at the highest level of theory employed. This survey is based on geometries of stationary points that were optimized at the DF-LCCSD(T)/def2-TZVPP level of theory (see previous section and Figure 3). The CCSD(T)/def2-QZVPP single-point energy calculations of these DF-LCCSD(T)/def2-TZVPP optimized geometries provide our reference energies and are collected in Table 2, reported as formation energies relative to the free isolated species LAu + N + A. We refer to these reference energies as CCSD(T)/def2-QZVPP//DF-LCCSD(T)/def2-TZVPP. In order to gain an estimation of the basis set

dx.doi.org/10.1021/ct400980w | J. Chem. Theory Comput. 2014, 10, 1021−1034

Table 2. Energy of the Selected Structures (in kcal/mol) Calculated at CCSD(T)/def2-QZVPP Level of Theory with Respect to Noninteracting Fragments ClAu + NH_3 + C_2H_2 and PAu^+ + NH_3 + C_2H_2 Taken As Zero Reference Energy[a]

	formation energy (kcal/mol)	
	L = Cl	L = P
LAuN	−45.9	−58.6
LAuAN	−49.6	−59.0
LAuA	−40.1	−41.7
LAu_TS	−28.9	−46.6
LAu_p1	−41.8	−71.4
LAu_p2	−81.6	−95.2

[a]All geometries optimized at DF-LCCSD(T)/def2-TZVPP.

incompleteness error using this reference basis set, we carried out a two-point extrapolation (def2-TZVPP/def2-QZVPP) procedure and an analysis of the basis set superposition effect (BSSE). For the two-point extrapolation, we used the Martin and Karton[82] formula for HF energy and the Truhlar[83] for the correlation. We found that the energies of all structures obtained from this extrapolation procedure are systematically stabilized by about 1 kcal/mol. The ClAuAN and LAu_p2 species present respectively the highest and the lowest stabilization (1.2 and 0.7 kcal/mol, respectively). The evaluation of the basis set superposition effect, estimated by the counterpoise correction procedure of Boys and Bernardi,[84] gives a contribution of the same order of magnitude as, but in the opposite direction of, the extrapolation procedure. Note that a similar phenomenon has been observed previously.[33] The largest effect was found in the case of ClAuAN, where the counterpoise correction reduces the formation energies of 1.6 kcal/mol. Mentel and Baerends reported a detailed discussion on the opportunity of the use of the counterpoise corrected bond energies showing that they may deviate more from the basis set limit numbers than uncorrected bond energies.[85] All of the energies presented in the following do not include corrections for the BSSE.

The energy profiles for both ClAu and PH_3Au^+ are characterized by the formation of stable LAuN, LAuAN, and LAuA complexes, which lead via the transition state for nucleophilic attack LAu_TS to the LAu_p1 product and successively to the very stable protodeauration product LAu_p2. The species containing PAu^+ are more stable than those with AuCl, but interestingly enough this stabilization is not systematic. The Au−N bond is about 10 kcal/mol stronger in PAu than in ClAu complexes and, more generally, the charged metal fragment, in comparison with the neutral species, shows a pronounced preference for coordinating a hard ligand such as ammonia or a carbanionic species rather than a C−C bond in η^2 mode. Consequently, while PAuA is only 1.6 kcal/mol more stable than ClAuA, the tricoordinated system PAuAN is 9.4 kcal/mol more stable than ClAuAN and PAuN is 12.7 kcal/mol more stable that ClAuN. The other reaction stationary points containing a more or less complete gold-σ-carbon are systematically even more stabilized for L = PH_3, so much that the transition state PAu_TS turns out to be at a lower energy than PAuA.

One further closely related observation can be made: the tricoordinated species ClAuAN and PAuAN are more stable than the noninteracting ClAuN + A and PAuN + A species by 3.7 and 0.4 kcal/mol, respectively, and their stability relative to ClAuA + N and PAuA + N is even larger: 9.5 and 17.3 kcal/mol, respectively. Contrasting this stability, the tricoordinated species should be entropically disfavored with respect to LAuN + A, which increases their Gibbs free energy of formation. However, our results in Table 2 suggest that these tricoordinated species should not be neglected in the computational studies of gold-catalyzed reactions, particularly when the role of the central barrier, that is the difference in energy between the TS and the reactant complex, which becomes decisive for the rate of chemical reactions in the high-pressure regime, is addressed. [A more realistic reaction profile for the PH_3Au+ complex would require the inclusion of a second NH_3 molecule which performs the nucleophilic attack to the tricoordinated species PAuAN. A full investigation of this point is beyond the scope of the present work.]

As above for the geometries, the energies of the stationary points were computed in a series of calculations using the following hierarchy of quantum chemical methods in combination with a def2-TZVPP Gaussian-type basis set: MP2, DF-LCCSD, and DF-LCCSD(T). Note that for each method we use consistently the geometries optimized with that method. Furthermore, based on DF-LCCSD(T)/def2-TZVPP geometries, the energies of stationary points were computed with single-point calculations at the canonical CCSD(T)/def2-TZVPP level, and based on the DF-LCCSD(T)/def2-SVP geometries, energies of the stationary points were computed with single-point calculations at the CCSD(T)/def2-SVP level. The statistical results (mean error (ε_e), standard deviation (σ_e), and maximum absolute error (M_e)) of ab initio calculations of energies (in kcal/mol) are summarized in Figure 4, while in

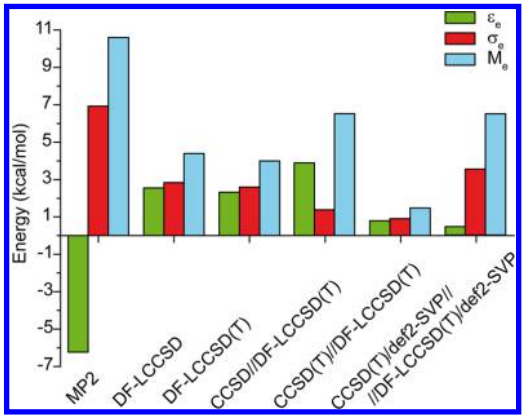

Figure 4. Mean error (ε_e), standard deviation (σ_e), and maximum absolute error (M_e) of the energies calculated with different ab initio methods [reference: CCSD(T)/def2-QZVPP//DF-LCCSD(T)/def2-TZVPP] setting the energy of isolated LAu + N +A species as zero reference energy. In all cases, the maximum absolute error occurs for ClAuAN.

Figure 5 the data are reported as a deviation from the reference data obtained at the CCSD(T)/def2-QZVPP level. If not specified otherwise, the basis set used is def2-TZVPP.

As found for the geometry optimizations, the MP2 method is inaccurate also for the energies. All the MP2 complexation energies, in particular those of the tricoordinated LAuAN and PAu_p2 species, are substantially larger (negative deviation) than the corresponding reference values. The maximum M_e is of about 10 kcal/mol for ClAuAN. Despite the MP2 method being still widely used in computational chemistry, our analysis shows clearly that this method is insufficient to gain accurate predictions for benchmarking in the field of gold chemistry. Several previous works achieved similar conclusions.[33,37,86,87] An improvement is

dx.doi.org/10.1021/ct400980w | J. Chem. Theory Comput. 2014, 10, 1021−1034

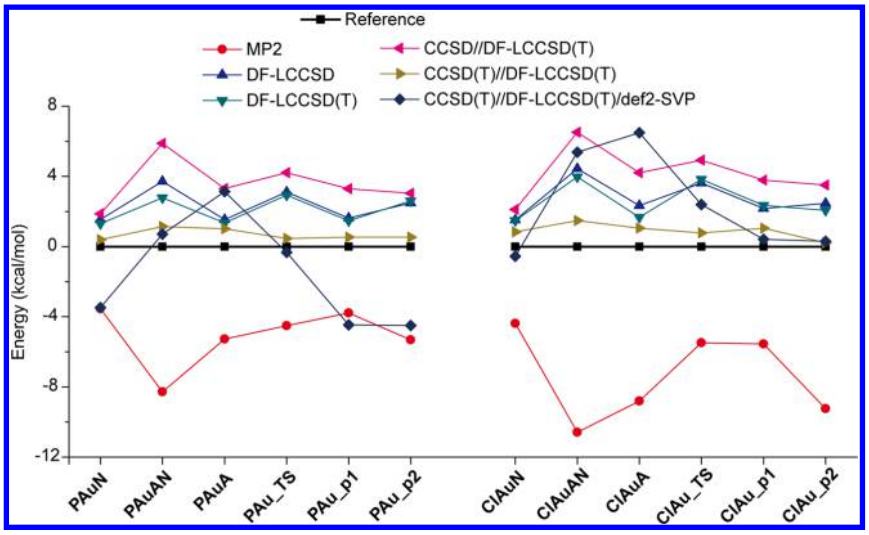

Figure 5. Deviations in the formation energy of different selected structures for $[PH_3Au]^+$ (left) and [ClAu] (right)—catalyzed ethyne hydroamination by ammonia computed with different ab initio methods. The reference energy values at the CCSD(T)/def2-QZVPP//DF-LCCSD(T)/def2-TZVPP level of theory are highlighted as a black line. Noninteracting LAu + N + A species are taken as zero-point energy.

Table 3. Mean Error (ε_r), Standard Deviation (σ_r), and Maximum Absolute Error (M_r) of the Au−Cl, Au−P, Au−C, and C−C Bonds[a]

	Au−Cl			Au−P			Au−C			C−C		
	ε_r	σ_r	M_r	ε_r	σ_r	M_r	ε_r	σ_r	M_r	ε_r	σ_r	M_r
6-31G**	7.6	1.1	9.7 ClAuAN	6.4	1.1	8.3 PAu_p1	4.2	3.2	9.0 PAuAN	−0.6	0.9	1.7 PAu_TS
def2-SVP	4.1	0.3	4.6 ClAuAN	5.1	0.9	6.6 PAuAN	2.9	1.3	6.0 PAu_TS	−0.2	0.6	1.4PAu_TS
def2-TZVP	2.5	0.4	3.4 ClAuAN	1.7	0.4	2.1 PAu_p1	2.9	1.1	4.2 PAu_TS	−1.0	0.9	2.2 PAu_TS
def2-TZVPD	2.6	0.6	3.8 ClAuAN	1.7	0.4	2.1 PAuA	1.7	1.8	3.9 PAu_TS	−0.5	1.1	2.1 PAu_TS
def2-QZVPP	2.1	0.7	3.4 ClAuAN	1.0	0.4	1.5 PAu_p1	1.5	1.6	3.5 ClAuAN	−1.3	0.5	2.2 PAu_TS

[a]Distances are in pm. The species M_r is relative to is also indicated.

obtained by using the LCCSD method with a large basis set, def2-TZVPP, with the complexation energies being underestimated by about 4 kcal/mol for the tricoordinated species. Here, ε_e is larger than 2 kcal/mol, but also σ_e is high (about 3 kcal/mol), a clear indication that the difference is not due only to a systematic error. The inclusion of the triple excitation in the local Coupled Cluster (DF-LCCSD(T)) improves slightly the description of the tricoordinated species, but the advantage in terms of accuracy on the overall energy profile is very limited, as shown by the statistical parameters. It is remarkable that the triple excitation effect included in the canonical method (CCSD(T)) gives a very important contribution. All statistical parameters are indeed improved shifting form 3.9, 1.4, and 6.5 to 0.9, 1.0, and 1.2, respectively, for ε_e, σ_e, and the largest error M_e. The importance of including triple excitations in the coupled cluster calculations to obtain accurate data has been recently pointed out by Nava et al.[34] in some related gold(I) systems. Moreover, on comparing energy results of DF-LCCSD(T)/def2-TZVPP with those of CCSD(T)/def2-TZVPP, i.e., using the same basis set quality on the same optimized structures, we see that canonical CCSD(T) yields significantly better results. The complexation energies are underestimated by only about 1 kcal/mol, and the description of both the LAuAN and LAu_TS systems improve compared to the local approach. The average error for the latter is below 1 kcal/mol and, more interestingly, the σ_e is halved with respect to DF-LCCSD(T). By contrast, CCSD(T) with a small basis set (def2-SVP) performs poorly, also resulting in large nonsystematic errors. Finally, we observe that the tricoordinated species ClAuAN, systematically exhibiting the largest error M_e, results in the most difficult species to describe in terms of energy.

Validation of DFT Methods. *Basis Set Convergence.* Most computational DFT studies in the literature on gold(I)-catalyzed reaction mechanisms have been performed using the very popular B3LYP functional with a 6-31G(d) (or 6-31G*) basis set and a LANL2DZ or SDD pseudopotential for gold to account for relativistic effects. This is not without problems, because, contrary to expectations of a relatively weak basis set dependence for DFT, it has been shown that B3LYP basis set effects may in general be large. For example, the deviation from the basis-set-converged value for the activation energy of transition-metal-catalyzed reactions can exceed 10 kcal/mol with a small basis set (6-31G**).[46,88] To begin investigating these basis set effects, we have optimized the geometries of all our stationary points using the B3LYP functional in conjunction with five different GTO basis sets, namely the Pople basis set 6-31G**, the Ahlrichs basis sets def2-SVP, def2-TZVP, def2-TZVPD, and def2-QZVPP. The results for the Au−Cl, Au−P, Au−C, and C−C bond lengths have been statistically analyzed using as a reference the limit basis set def2-QZVPP, and the mean error (ε_r), standard deviation (σ_r), and maximum absolute error (M_r) are reported in Table 3.

The C−C bond distance turns out to be very robust with respect to changing the basis set, with small ε_r and σ_r values, and maximum errors between 1.4 and 2.2 pm. For the Au−Cl, Au−P, and Au−C bond lengths, the 6-31G** basis set is not sufficiently accurate in reproducing the benchmark geometries, with maximum errors in the range 8−10 pm. Note that the use of a larger basis set substantially improves all the statistic parameters,

dx.doi.org/10.1021/ct400980w | J. Chem. Theory Comput. 2014, 10, 1021−1034

with the def2-TZVP basis set already giving sufficiently accurate results. Adding a diffuse function (def2-TZVPD) or increasing the basis set size using def2-QZVPP slightly improves the performance. The most problematic species are the tricoordinated PAuAN and ClAuAN and the transition states PAu_TS. This is in line with the fact that in these species bonds are being broken along the reaction coordinate, which causes more pronounced sensitivity to changes in the basis set quality (and functional type).

A statistical analysis of the relative energies calculated with the B3LYP functional and the five chosen basis sets is displayed in Figure 6. The reference values are those obtained using the limit

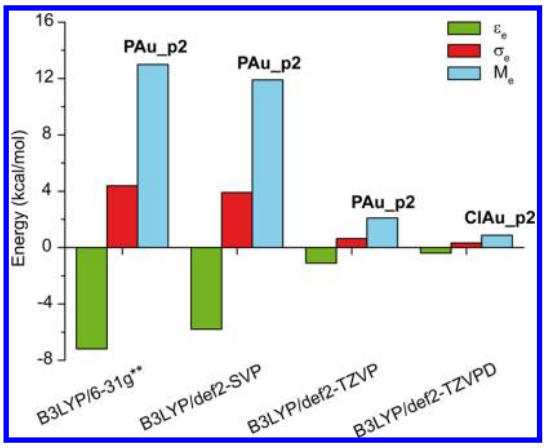

Figure 6. Mean error (ε_e), standard deviation (σ_e), and maximum absolute error (M_e) of the energies calculated with B3LYP in combination with different basis sets. The reference values have been obtained at B3LYP in combination with def2-QZVPP.

basis set def2-QZVPP. We observe again that the 6-31G** basis set does not give accurate results, similarly to the def2-SVP basis. Almost converged data can be obtained using the def2-TZVP basis with an average error of about 1 kcal/mol and a small standard deviation. Adding a diffuse function to the basis set (def2-TZVPD) or increasing the basis set size (def2-QZVPP) is only marginally beneficial for the energy calculations. Similar conclusions have been achieved recently by Chen et al.[33,88−90] As we will show in the following, the typical errors that one may expect using different DFs are significantly larger. These results show that the widely used B3LYP hybrid functional needs to be used in conjunction with basis sets larger than 6-31G** in order to achieve satisfactorily converged result (at least the def2-TZVP basis set).

Performance of Different DF Approximations. Having established that the def2-TZVP gives a sufficiently accurate basis set, we used it to analyze both the geometries and the relative energies of our stationary point structures computed with a few popular DF approximations, namely the GGA functionals BLYP, OPBE, and BP86; the meta-GGA functional M06-L; the hybrid functionals PBE0 and B3LYP; the meta-hybrid functionals M06 and TPSSh; and the double-hybrid functional B2PLYP. The performance of the different functionals on the geometries is assessed by a statistical comparison of the optimized Au−Cl, Au−P, Au−,C and C−C bond lengths with our DF-LCCSD(T)/def2-TZVPP benchmark. The statistical parameters (mean error ε_r, standard deviation σ_r, and maximum absolute error M_r) are reported in Table 4.

All of the investigated DFs show a nice agreement with the benchmark results, with mean errors in the range between +4.2 and −3.7 pm, the standard deviation between 1.9 and 0.3, and maximum absolute error between 6.8 and 0.2 pm. The Au−C distance is the most difficult geometrical parameter to converge, presenting both the largest σ_r and largest M_r. Among GGA functionals, we can underline the good performance of BP86. It gives results close to those one can obtain using the hybrid PBE0 and meta-hybrid TPSSh and even better than B3LYP. Note that the meta-hybrid M06 gives quite poor statistical results with a M_r of 6.7 pm for the Au−C distance of the tricoordinate structure (PAuAN). The best performance here is obtained with the double-hybrid functional B2PLYP. However, provided that a sufficiently large basis set is used, we may conclude that the geometries obtained with the various DFs all agree well with each other and, with only few exceptions, with the benchmark DF-LCCSD(T)/def2-TZVPP results.

We now proceed to examine the performance of the different DFs for the energies by comparing the results with those calculated in our ab initio benchmark. For each DF, we use the geometries optimized with that functional. The deviation in the computed energies using the various DFs in combination with the def2-TZVPP basis set with respect to the reference calculation (CCSD(T)/def2-QZVPP//DF-LCCSD(T)/def2-TZVPP) are reported in Figure 7. The relative statistical analysis on the data set obtained including all reference structures (Figure 3) is reported in Figure 8 as ε_e, σ_e, and M_e.

The behavior of the considered DFs in computing the formation energies is alarming. Most of the DFs present important nonsystematic deviations. Furthermore, the pattern

Table 4. Mean Error (ε_r), Standard Deviation (σ_r), and Maximum Absolute Error (M_r) of the Au−Cl, Au−P, Au−C, and C−C Bond Lengths Optimized with Various DFs Using def2-TZVPP Basis Set (Benchmark: DF-LCCSD(T)/def2-TZVPP)[a]

	Au−Cl			Au−P			Au−C			C−C		
	ε_r	σ_r	M_r	ε_r	σ_r	M_r	ε_r	σ_r	M_r	ε_r	σ_r	M_r
BLYP	4.2	0.6	5.4 ClAuAN	2.8	0.6	3.6 PAu_p1	4.2	1.6	6.7 PAu_TS	−0.1	0.5	1.4 PAu_TS
OPBE	−2.1	0.5	0.8 ClAu	−3.0	1.0	4.0 PAuAN	−3.7	1.9	6.8 PAuA	0.5	0.7	1.3 ClAu_p2
BP86	0.9	0.5	1.6 ClAuAN	0.0	0.7	1.2 PAu	0.4	1.5	3.1 PAu_TS	0.2	0.7	1.3 ClAu_p2
M06-L	2.4	0.8	3.7 ClAuAN	0.5	0.5	1.2 PAuA	0.7	1.5	3.6 PAu_TS	−0.9	0.5	2.0 PAu_TS
B3LYP	2.5	0.4	3.4 ClAuA	1.7	0.4	2.1 PAu_p1	2.9	1.1	4.2 PAu_TS	−1.0	0.9	2.2 PAu_TS
PBE0	−0.3	0.3	0.8 ClAuA	−0.7	0.5	1.5 PAu_p1	−0.9	1.1	2.4 PAuA	−1.1	0.5	2.0 PAu_TS
M06	2. 5	0.3	2.9 ClAu	3.6	0.4	4.2 PAu	3.6	1.4	6.7 PAuAN	−1.6	0.4	2.3 ClAu_TS
TPSSh	0.5	0.5	1.4 ClAuAN	−0.4	0.5	1.1 PAu	−0.4	1.4	2.2 PAuAN	−0.6	0.6	0.2 PAu_TS
B2PLYP	0.8	0.3	1.2 ClAuAN	−0.4	0.4	0.9 PAuAN	−0.1	0.8	1.3 PAuAN	−0.7	0.4	1.4 PAu_TS

[a]Distances are in pm. The species corresponding to M_r is also indicated.

dx.doi.org/10.1021/ct400980w | J. Chem. Theory Comput. 2014, 10, 1021−1034

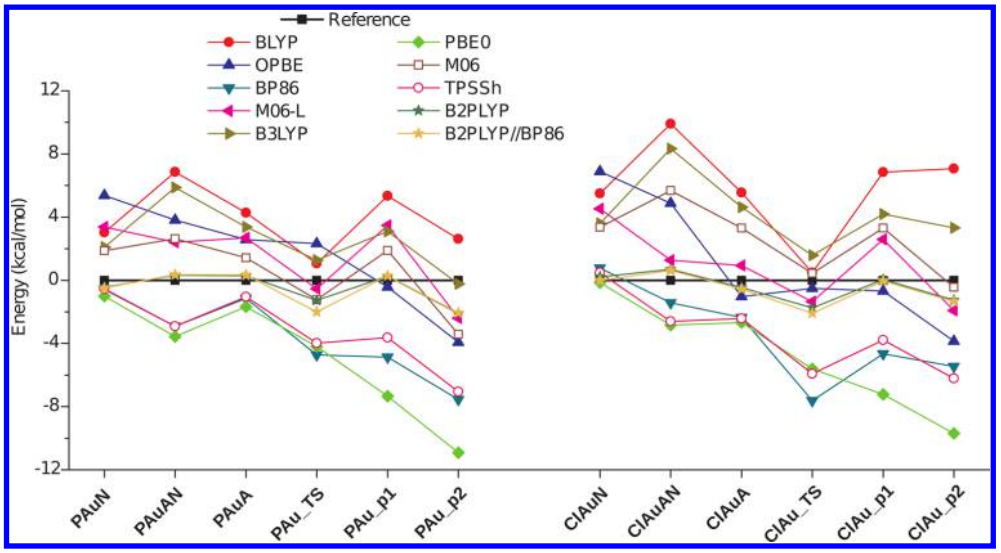

Figure 7. Deviation in formation energy of the complexes obtained with different DFT methods in combination with the def2-TZVP basis set. The deviation is reported with respect to the reference energy (CCSD(T)/def2-QZVPP//DF-LCCSD(T)/def2-TZVPP) setting the energy of isolated LAu + N +A species as zero-point energy.

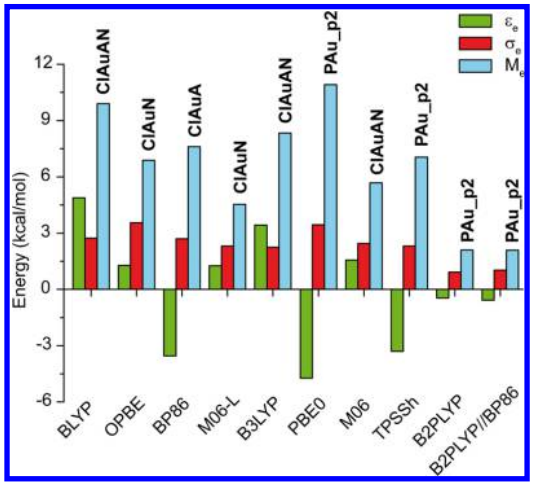

Figure 8. Mean error (ε_e), standard deviation (σ_e), and maximum absolute error (M_e) of the energies calculated with different DFT methods in combination with the def2-TZVP basis set [reference: CCSD(T)/def2-QZVPP//DF-LCCSD(T)/def2-TZVPP] setting the energy of isolated LAu + N +A species as zero-point energy. The species corresponding to M_e is also indicated.

of these deviations (Figure 7) is strongly dependent on the DF employed. We mention the example of two hybrid DFs: PBE0 gives almost an exact prediction for the PAuN but overestimates (by about 12 kcal/mol) the stability of the final product (PAu_p2); B3LYP shows high accuracy in predicting the energy stabilization of the product (PAu_p2) but underestimates the stability of the tricoordinated species (PAuAN) by about 6 kcal/mol. The statistical parameters show a spread in ε_e of 12 kcal/mol (with values between −7 and +5 kcal/mol) and absolute M_r values ranging from 4 to 12 kcal/mol. This clearly demonstrates the necessity of a careful selection of DF, even when a large basis set is used. We note that the GGA functional OPBE, the meta-GGA functional M06-L, and the meta-hybrid functional M06 present a ε_e close to the CCSD(T)/def2-QZVPP benchmark, but these apparent good performances are clearly due to nonsystematic errors that cancel out in the averaged ε_e (see Figure 7). This is clearly indicated by the large values of σ_e, respectively 3.5, 2.3, and 2.4 kcal/mol, which are similar to others DFs.

The best performance is clearly observed for the double-hybrid B2PLYP functional with an ε_e value lower than 1 kcal/mol combined with a small σ_e (about 1 kcal/mol) and an absolute M_e value of 2 kcal/mol, corresponding to a very small relative error of less than 2%. A drawback in the applicability of this functional in routine calculations is clearly its computational cost, because the extra second-order perturbation correlation involving virtual orbitals effectively scales as MP2. However, it is important to note that a full geometry optimization is not necessary here, and the statistical performance remains almost totally unchanged even if one uses the double-hybrid B2PLYP functional in a single point calculation on optimized structures obtained using the much more computationally efficient GGA DFs. As a demonstration, we included in Figures 7 and 8 the data obtained by such calculation, where we use double-hybrid B2PLYP in a single point energy on the geometries obtained at BP86. This approach is referred to as B2PLYP//BP86 in Figure 8.

Among the complexes we included in the statistics, the most difficult to treat by different DFs approximations is the tricoordinated species. In this case, the relative error may be as large as 30%. A cautionary remark should be made regarding the stability of these tricoordinated LAuAN compared to biscoordinated LAuN + A and LAuA + N species. The results are summarized in Table 5. Most of the considered DFT functionals give a tricoordinated species even more stable than the LAuN + A, as the CCSD(T)/def2-QZVPP//DF-LCCSD(T)/def2-TZVPP benchmark method does. But, remarkably, this is not the case for the B3LYP and BLYP functionals, which underestimate the stability of PAuAN relative to [PAuN + A] by nearly 4 kcal/mol and that of ClAuAN relative to [ClAuN + A] by well over 4 kcal/mol.

This unsatisfactory description of the relative energy of tricoordinated vs biscoordinated may have implications for the widely accepted strategy of performing a geometry optimization at, say, the B3LYP/6-31G** level and subsequently refining the energies by single point calculations at a higher level of theory. Since this functional is the most used for preliminary calculations, this can be the reason why reaction paths that involve

dx.doi.org/10.1021/ct400980w | J. Chem. Theory Comput. 2014, 10, 1021−1034

Table 5. Energy Difference (kcal/mol) between the Tricoordinated Species LAuAN and the Biscoordinated LAuN+A and LAuA+N, Respectively Referred to As ΔE_N and ΔE_A[a]

	ΔE_N		ΔE_A	
DF	L = PH_3	L = Cl	L = PH_3	L = Cl
BLYP	3.4	0.7	−14.7	−5.2
OPBE	−2.0	−5.7	−16.1	−3.6
BP86	−2.7	−5.6	−19.1	−8.6
M06-L	−1.4	−6.9	−17.6	−9.2
B3LYP	3.4	1.0	−14.8	−5.8
PBE0	−3.0	−6.7	−19.2	−9.7
M06	0.4	−1.4	−16.1	−7.2
TPSSh	−2.8	−6.8	−19.2	−9.7
B2PLYP	0.4	−3.2	−17.3	−8.4
B2PLYP//BP86	0.4	−3.1	−17.3	−8.3
ref.	−0.4	−3.7	−17.3	−9.5

[a]Results reported for different density functionals (DF).

tricoordinated species are scarcely considered.[27] Lledòs and co-workers[27] calculated a ΔE of −12 kcal/mol between their model system {[(carbene)Au(NH3)] + 2-butyne} (the most stable species) and [(carbene)Au(NH3)(2-butyne)], and indeed they used the B3LYP/SDD-6-31G(d) method for optimization and M06/SDD-6-311++G(d,p) method for single-point calculation of the energy, both of which give a negative ΔE, favoring the linear biscoordinated LAuN structure over the tricoordinated one. The risk in using B3LYP and BLYP functionals in computational studies of Au(I)-catalyzed alkyne hydroamination reactions is that some of the highly branched paths, expecially involving tricoordinated species, in the mechanisms could be missed.

A further issue that arises in the evaluation of the performance of different DFs considering different structures along a suitable reaction path, as we have done here, is that the statistics, and the conclusions drawn from them, may be influenced by the choice of the reference energy, since the errors affecting this reference point are effectively neglected in the analysis. This simple question was largely unexplored in previous benchmark investigations but may be important for the purpose of assessing the performance of different functionals. As pointed out above, we have analyzed the energies of the stationary point structures with respect to the noninteracting fragments ClAu + N + A and PAu + N + A taken as zero-point energy (Figures 7 and 8). An alternative reference structure may be the (LAuN + A) asymptote, which may be considered a "natural" choice to examine the formation of the tricoordinated species. With this reference, the statistical analysis results are shown in Figure 9 (left panel). The choice of a reference cancels, by definition, the error in the reference structure, and this may modify significantly the statistical results. While, for instance, hybrid B3LYP and the GGA BLYP seems to improve substantially, presenting a really low ε_e value (lower than 1 kcal/mol) and a M_e reduced up to less than 5 kcal/mol, the OPBE functional gets worse and decreses ε_e from less than 1.5 kcal/mol up to almost −6 kcal/mol, and ε_e passes from 7 to 11 kcal/mol. Note that in both cases the precision is not improved significantly as shown by the values of σ_e, which remain really stable with the change of the zero-energy reference. The best DF is the double-hybrid B2PLYP with really stable statistical parameters: ε_e value lower than 1 kcal/mol with σ_e of about 1 kcal/mol.

As a further option, the energy of the tricoordinated species LAuAN can be taken as a reference. Since these are more stable than biscoordinated, these species may open additional paths in the reaction mechanism investigation. The statistical analysis has been repeated choosing the LAuAN as the zero-point energy, and the functionals that are more accurate for the energy calculation of tricoordinated LAuAN species are highlighted on the basis of the results depicted in Figure 9 (right panel). The meta-hybrid TPSSh and meta-GGA M06-L functionals perform very similarly and improve the statistical parameters. In this case, the ε_e is reduced below 1 kcal/mol, and M_e is less than 5 kcal/mol, but here the standard deviation is slightly increased up to 2.5 kcal/mol in both cases. Note that the statistics of B3LYP change significantly due to the error cancellation that arises by the use of LAuAN energy as zero energy. Here, while the ε_e is significant (about 4.5 kcal/mol), the deviations are more systematic, as shown by the important reduction of σ_e that now is 1.34 kcal/mol. The B2PLYP performances are again really stable with ε_e increasing slightly but remaining below 1 kcal and a σ_e of 0.9 kcal/mol. In all cases, independently by the zero energy reference, the single point energy calculation using B2PLYP on BP86 optimized structures (B2PLYP//BP86) gives almost

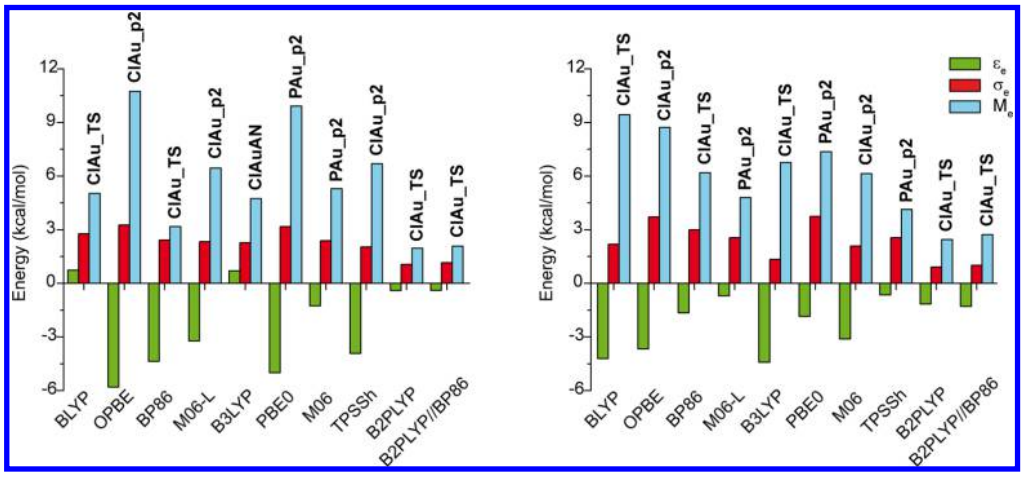

Figure 9. Mean error (ε_e), standard deviation (σ_e), and maximum absolute error (Merr) of the energies computed with different DFT functionals in combination with def2-TZVPP basis set [reference: DF-LCCSD(T)/def2-TZVPP//CCSD(T)/def2-QZVPP] with the energy of LAuN + A (left panel) and LAuAN (right panel) taken as zero-point energy.

dx.doi.org/10.1021/ct400980w | J. Chem. Theory Comput. 2014, 10, 1021−1034

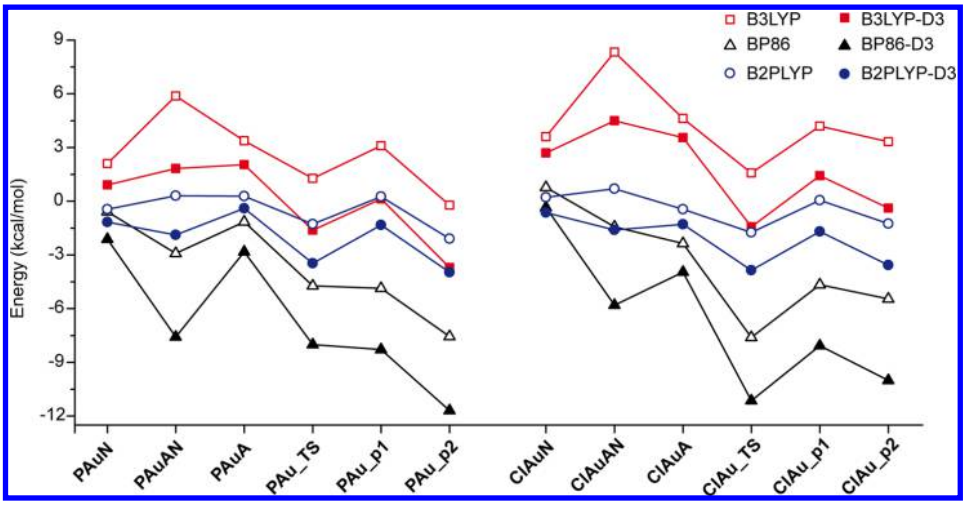

Figure 10. Deviation in formation energy of the complexes obtained with different DFT methods in combination with the def2-TZVP basis set. The deviation is reported with respect to the reference energy (CCSD(T)/def2-QZVPP//DF-LCCSD(T)/def2-TZVPP), setting the energy of isolated LAu + N +A species as zero-point energy.

exactly the same statistical parameters. We mention that the good performance of the double-hybrid functional as B2PLYP for the description of Au(I)/Au(III) complexes with unsaturated molecules was already pointed out by Chen et al.[33]

In Figure 10, we compare the results for three representative functionals, namely, BP86, B3LYP, and B2PLYP, after adding a DFT-D3 dispersion correction.[91] The inclusion of dispersion correction increases the formation energy, but this stabilization is not systematic along the reaction path and does not always improve the performance of the functional. In all cases, the largest contribution is found for the tricoordinated species (PAuAN and ClAuAN). In the case of the BP86 functional, the inclusion of dispersion gives even a significant deterioration of the statistical parameters for both the average (ε_e) and maximum error (M_e). Their values pass indeed from −3.5 and 7.6 of BP86 to −6.6 and 11.7 kcal/mol of BP86-D3. For this functional also, the standard deviation increases significantly, passing from 2.7 to 3.7 kcal/mol.

The inclusion of dispersion effects in B3LYP-D3 improved significantly both ε_e and M_e, but this improvement does not reflect an increase of the precision of the predictions. Here, indeed, the standard deviation slightly deteriorates passing from the 2.2 of B3LYP to the 2.3 kcal/mol of B3LYP-D3. Despite a light deterioration of the performance of the B2PLYP functional due to the inclusion of the dispersion effect (the statistical parameters passed from −0.6, 1.0, and 2.1 of B2PLYP to −2.1, 1.3, and 4.0 of B2PLYP-D3, respectively for ε_e, σ_e, and M_e), it remains to be the most accurate functional.

Benchmark on Relativistic Approximations. In the work described in the previous sections, we included relativistic effects at the scalar level using relativistic effective core potentials (RECP) on the gold atom. But other methods, based on all-electron calculations, are often used. A notable example, employed in transition metal chemistry, for including scalar relativistic effect is the all-electron ZORA approach. Furthermore, current knowledge of nonscalar relativistic effects, like spin−orbit coupling, on different intermediates along a reaction path involving a heavy-metal catalyst is very limited. Here, we present a quantitative investigation of the effect of different approximations on a reaction energy profile involving gold(I) catalysts. As a reference, we use the full relativistic Dirac−Kohn−Sham approach based on the four-component Dirac equation. This approach includes both scalar and nonscalar terms (e.g., spin−orbit) at the most rigorous level.

We now compare the fully relativistic DKS complexation energies with the results obtained by RECP and all-electron ZORA calculations, using in all cases the BP86 DF and the reference structures obtained at the DF-LCCSD(T)//def2-TZVPP level. The results are reported in Figure 11. The

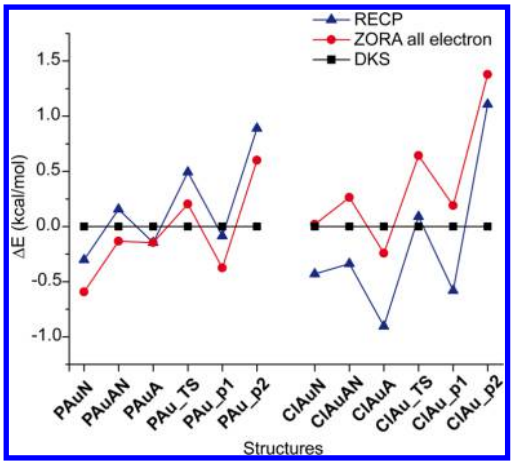

Figure 11. Energy deviation in kcal/mol in the complexation energy using different Hamiltonians: relativistic effective core potential (RECP), ZORA all electrons. The reference value is obtained by all electron Dirac−Kohn−Sham (DKS) calculations with a limit basis set. The exchange-correlation functional used is BP86. The stuctures used in calculations are the reference structure obtained at DF-LCCSD(T)//def2-TZVPP. See text for details.

reference value (zero line in the figure) is obtained by all electron Dirac−Kohn−Sham (DKS) calculations with a limit basis set. In order to minimize the effects of basis set incompleteness, we have used a large basis, as close to the limit as possible. In the case of the RECP calculation, we used the limit basis of the def2 family, namely, def2-QZVPP.[54] The calculations using the ZORA Hamiltonian have been done with the ADF program (ADF2010.01) using the all-electron QZVPP Slater-type basis.[63] The DKS calculations have been carried out with the DKS module of the fully relativistic code BERTHA. In this case,

dx.doi.org/10.1021/ct400980w | J. Chem. Theory Comput. 2014, 10, 1021−1034

the large component basis set has been obtained by decontracting the def2-QZVPP basis set on hydrogen, carbon, nitrogen, and phosphorus, while the limit quadruple-ζ quality basis sets (34s30p19d12f3g1h) by Dyall have been used for the gold atom.[68,69] The corresponding small-component basis was generated using the restricted kinetic balance relation.[70] Further details of this approach can be found in ref 64.

The results show that both ZORA and RECP present very similar deviation patterns along the reaction energy profile for both the AuCl and PH_3Au^+ catalysts. Besides the absolute deviation, which may be affected by residual basis set incompleteness, the deviation in the description of the energy profile of a reaction is expected to be really small. The discrepancy with respect to the reference DKS results is below 1.5 kcal/mol. It is interesting to consider the effect of the Hamiltonian on the activation energy defined as the difference between ΔE(LAuA) and ΔE(LAu_TS). We found here that nonscalar effects are not completely negligible. In particular, the transition state PAu_TS is destabilized with respect to biscoordinated PAuA by 0.65 and 0.35 kcal/mol using RECP and ZORA calculations, respectively. In the case of ClAu_TS, this destabilization is of 0.99 and 0.89 kcal/mol, respectively. We mention that an effect of a similar size but of opposite sign was observed recently by Chen et al. in the case of the reaction of C−H activation by Pt(II).[39]

CONCLUSIONS

In conclusion, in the present study, we have computed an ab initio benchmark for an archetypal gold(I)-catalyzed hydroamination of ethyne employing a hierarchical series of methods and basis sets up to CCSD(T)/def2-QZVPP and DF-LCCSD(T)/def2-TZVPP, focusing on both geometries and energies. We studied up to 12 structures of possible Au(I)-coordinated species modeling different intermediates potentially present in a catalytic cycle for the addition of a protic nucleophile to an alkyne. Our findings have evidenced the importance of sufficiently large basis sets in coupled cluster calculations for obtaining reliable energies as well as the low accuracy of MP2. The reference structures of different stationary points of the reaction energy profile reveal peculiar details of coordination features depending on whether the gold(I) catalyst is a neutral AuCl or an ionic $[PH_3Au]^+$.

The benchmark is used to evaluate the performances of some popular density functionals for describing geometries and relative energies of stationary points along the reaction profile. The minimum acceptable GTO basis set for these DFT calculations is found to be of triple-ζ quality with polarization on all atoms, such as def2-TZVP. For geometries, it was found that most of the investigated GGA; meta-GGA; as well as hybrid, double-hybrid, and meta-hybrid DFT approaches provide an accurate description when used in combination with converged basis sets. Much more challenging is it to achieve accurate results for the energy. Most functionals (including hybrid or meta-hybrid) give nonsystematic errors along the reaction profile, with a spread of 4−12 kcal/mol. We have also investigated the impact of the choice of the reference system used to define the energy zero. Particularly challenging is a description of the tricoordinated complexes. In this case, the hybrid B3LYP underestimates our reference data up to 9 kcal/mol.

The double hybrid functional B2PLYP outperforms all other considered functionals and compares very nicely with our reference ab initio benchmark energies. It presents both small absolute errors and, crucially, a very small standard deviation (about 1 kcal/mol). The major drawback with B2PLYP is that it is more computationally expensive than other functionals (e.g., GGA, hybrid, meta-hybrid) due to the second-order perturbation correlation involving virtual orbitals. It effectively scales as a MP2-like term. We found that a single point energy calculation on optimized structures at a less expensive GGA level gives almost identical results and statistical parameters as one may achieve if the structures would be fully relaxed at the B2PLYP level. Further, when combined with a Laplace transformation type algorithm, the B2PLYP approach scales only as $O(N^4)$ with the system size.

We caution that, if the very accurate B2PLYP functional is not used for energy calculations, the reaction profile landscape may change unpredictably, opening or closing branched paths depending on the functional. In catalytic systems, the use of computationally less expensive, but less accurate, functionals may jeopardize the conclusions drawn in studies focusing on branched reaction paths in catalytic cycles. Notably, the common strategy of using the B3LYP functional in combination with a small basis set such as 6-31G* or 6-31-G** is inaccurate, and it can result, as a consequence, that important, rate determining paths in reactivity studies could be missed, in particular if a tricoordinated species is involved. On the basis of our investigations, the best density functional recipe for homogeneous gold catalysis turns out to be the following: geometry optimizations using GGA, meta-GGA, hybrid, or meta-hybrid functionals, since the various functionals do not show significant mutual discrepancies, in combination with a sufficiently large basis set (at least of triple-ζ type with polarization) followed by a single-point B2PLYP energy calculations on the optimized structures.

Finally, we assessed the accuracy of commonly used approaches to include relativistic effects, such as relativistic effective potentials and the ZORA Hamiltonian, by comparing the results with those of fully relativistic, all-electron, four-component DKS calculations, using limit basis sets in all calculations. We found that the scalar approximations yield reaction profiles essentially in agreement with each other to within 0.5 kcal/mol. Their deviation from the reference four-component results is however larger, ranging from 1 to 2 kcal/mol in the investigated systems. The error in the activation energy of the nucleophilic attack is less than 1 kcal/mol. Thus, while accounting for nonscalar relativistic effects is confirmed to be mandatory, in order to achieve truly quantitative accuracy, routine investigations of gold(I) catalyzed reaction mechanisms may achieve meaningfully reliable results also within scalar approximations.

While we have focused here only on prototypical reaction species involving homogeneous-phase gold(I) catalysts for the activation of UHCs, without any attempt to investigate all possible reaction paths, we believe that the benchmark assessments obtained and the general considerations that emerge from our study may be a useful basis for further investigations and for the definition of an efficient approach to study gold-catalyzed organic reactions.

ASSOCIATED CONTENT

Supporting Information

Energies and Cartesian coordinates of all reference species. This material is available free of charge via the Internet at http://pubs.acs.org

AUTHOR INFORMATION

Corresponding Authors

*E-mail: paola.belanzoni@unipg.it.
*E-mail: leonardo.belpassi@cnr.it.

Notes

The authors declare no competing financial interest.

ACKNOWLEDGMENTS

This work was supported by grants from the Italian MIUR and the FIRB-futuro-in-ricerca project: "Novel Au(I)-based molecular catalysts: from know-how to know-why (AuCat)," RBFR1022UQ. We thank the Italian SuperComputing Resource Allocation (ISCRA) through the project HP10BT1TD8 (BERTHA) for computational resources.

REFERENCES

(1) Hohenberg, P.; Kohn, W. *Phys. Rev.* **1964**, *136*, B864−B871.
(2) Kohn, W.; Sham, L. J. *Phys. Rev.* **1965**, *140*, A1133−A1138.
(3) Parr, R.; Yang, W. *Density-Functional Theory of Atoms and Molecules*; International Series of Monographs on Chemistry; Oxford University Press: New York, 1989.
(4) Harvey, J. N. *Annu. Rep. Prog. Chem. Sect. C: Phys. Chem.* **2006**, *102*, 203−226.
(5) Cramer, C. J.; Truhlar, D. G. *Phys. Chem. Chem. Phys.* **2009**, *11*, 10757−10816.
(6) Hashmi, A. S. K. *Chem. Rev.* **2007**, *107*, 3180−3211.
(7) Gorin, D. J.; Sherry, B. D.; Toste, F. D. *Chem. Rev.* **2008**, *108*, 3351−3378.
(8) Arcadi, A. *Chem. Rev.* **2008**, *108*, 3266−3325.
(9) Corma, A.; Leyva-Pèrez, A.; Sabater, M. J. *Chem. Rev.* **2011**, *111*, 1657−1712.
(10) Hashmi, A.; Toste, F. *Modern Gold Catalyzed Synthesis*; Wiley: New York, 2012.
(11) Wu, J.; Kroll, P.; Dias, H. V. R. *Inorg. Chem.* **2009**, *48*, 423−425.
(12) Brown, T. J.; Sugie, A.; Dickens, M. G.; Widenhoefer, R. A. *Organometallics* **2010**, *29*, 4207−4209.
(13) Hooper, T. N.; Green, M.; Russell, C. A. *Chem. Commun.* **2010**, *46*, 2313−2315.
(14) Sanguramath, R. A.; Hooper, T. N.; Butts, C. P.; Green, M.; McGrady, J. E.; Russell, C. A. *Angew. Chem., Int. Ed.* **2011**, *50*, 7592−7595.
(15) Ciancaleoni, G.; Belpassi, L.; Tarantelli, F.; Zuccaccia, D.; Macchioni, A. *Dalton Trans.* **2013**, *42*, 4122−4131.
(16) Salvi, N.; Belpassi, L.; Zuccaccia, D.; Tarantelli, F.; Macchioni, A. *J. Organomet. Chem.* **2010**, *695*, 2679−2686.
(17) Zuccaccia, D.; Belpassi, L.; Rocchigiani, L.; Tarantelli, F.; Macchioni, A. *Inorg. Chem.* **2010**, *49*, 3080−3082.
(18) Zuccaccia, D.; Belpassi, L.; Tarantelli, F.; Macchioni, A. *J. Am. Chem. Soc.* **2009**, *131*, 3170−3171.
(19) Brooner, R. E. M.; Brown, T. J.; Widenhoefer, R. A. *Chem.—Eur. J.* **2013**, *19*, 8276−8284.
(20) Zhdanko, A.; Ströbele, M.; Maier, M. E. *Chem.—Eur. J.* **2012**, *18*, 14732−14744.
(21) Young, P. C.; Green, S. L. J.; Rosair, G. M.; Lee, A.-L. *Dalton Trans.* **2013**, *42*, 9645−9653.
(22) Brooner, R. E. M.; Widenhoefer, R. A. *Angew. Chem., Int. Ed.* **2013**, *52*, 11714−11724.
(23) Lavallo, V.; Frey, G.; Donnadieu, B.; Soleilhavoup, M.; Bertrand, G. *Angew. Chem., Int. Ed.* **2008**, *47*, 5224−5228.
(24) Kovács, G.; Ujaque, G.; Lledòs, A. *J. Am. Chem. Soc.* **2008**, *130*, 853−864.
(25) Wang, W.; Hammond, G. B.; Xu, B. *J. Am. Chem. Soc.* **2012**, *134*, 5697−5705.
(26) Roithoá, J.; Hrusák, J.; Schröder, D.; Schwarz, H. *Inorg. Chim. Acta* **2005**, *358*, 4287−4292.
(27) Kovćs, G.; Lledoś, A.; Ujaque, G. *Angew. Chem., Int. Ed.* **2011**, *50*, 11147−11151.
(28) Pyykkö, P. *Chem. Rev.* **1988**, *88*, 563−594.
(29) Pyykkö, P. *Chem. Soc. Rev.* **2008**, *37*, 1967−1997.
(30) Toste, D. F.; Gorin, D. J. *Nature* **2007**, *446*, 395−403.
(31) Katari, M.; Rao, M. N.; Rajaraman, G.; Ghosh, P. *Inorg. Chem.* **2012**, *51*, 5593−5604.
(32) Hansmann, M. M.; Pernpointner, M.; Döpp, R.; Hashmi, A. S. K. *Chem.—Eur. J.* **2013**, *19*, 15290−15303.
(33) Kang, R. H.; Chen, H.; Shaik, S.; Yao, J. *J. Chem. Theory Comput.* **2011**, *7*, 4002−4011.
(34) Nava, P.; Hagebaum-Reignier, D.; Humbel, S. *ChemPhysChem.* **2012**, *13*, 2090−2096.
(35) Pašteka, L. F.; Rajskỳ, T.; Urban, M. *J. Phys. Chem. A* **2013**, *117*, 4472−4485.
(36) Rang, R. H.; Lai, W.; Yao, J.; Shaik, S.; Chen, H. *J. Chem. Theory Comput.* **2012**, *8*, 3119−3127.
(37) Faza, O.; Rodrǵuez, R.; López, C. *Theor. Chem. Acc.* **2011**, *128*, 647−661.
(38) Correa, A.; Marion, N.; Fensterbank, L.; Malacria, M.; Nolan, S.; Cavallo, L. *Angew. Chem., Int. Ed.* **2008**, *47*, 718−721.
(39) Chen, K. J.; Zhang, G.; Chen, H.; Yao, J.; Danovich, D.; Shaik, S. *J. Chem. Theory Comput.* **2012**, *8*, 1641−1645.
(40) Kim, J.; Hong, K.; Kim, H. K.; Lee, Y. S.; Kim, T. K. *J. Chem. Theory Comput.* **2013**, *9*, 1087−1092.
(41) Chen, H.; Kong, X.-Y.; Zheng, W.; Yao, J.; Kandalam, A. K.; Jena, P. *ChemPhysChem.* **2013**, *14*, 3303−3308.
(42) Kinjo, R.; Donnadieu, B.; Bertrand, G. *Angew. Chem., Int. Ed.* **2011**, *50*, 5560−5563.
(43) Ito, H.; Harada, T.; Ohmiya, H.; Sawamura, M. *Beilstein J. Org. Chem.* **2011**, *7*, 951−959.
(44) Patil, N. T.; Lakshmi, P. G. V. V; Singh, V. *Eur. J. Org. Chem.* **2010**, *2010*, 4719−4731.
(45) Piacenza, M.; Hyla-Kryspin, I.; Grimme, S. *J. Comput. Chem.* **2007**, *28*, 2275−2285.
(46) Kazaryan, A.; Baerends, E. J. *J. Comput. Chem.* **2013**, *34*, 870−878.
(47) Werner, H.-J.; Knowles, P. J.; Knizia, G.; Manby, F. R.; Schütz, M. *WIREs Comput. Mol. Sci.* **2012**, *2*, 242−253.
(48) Werner, H.-J.; Knowles, P. J.; Knizia, G.; Manby, F. R.; Schütz, M. Molpro version 2010.1, a package of ab initio programs. See http://www.molpro.net.
(49) Frisch, M. J.; Trucks, G. W.; Schlegel, H. B.; Scuseria, G. E.; Robb, M. A.; Cheeseman, J. R.; Scalmani, G.; Barone, V.; Mennucci, B.; Petersson, G. A.; Nakatsuji, H.; Caricato, M.; Li, X.; Hratchian, H. P.; Izmaylov, A. F.; Bloino, J.; Zheng, G.; Sonnenberg, J. L.; Hada, M.; Ehara, M.; Toyota, K.; Fukuda, R.; Hasegawa, J.; Ishida, M.; Nakajima, T.; Honda, Y.; Kitao, O.; Nakai, H.; Vreven, T.; Montgomery, J. A., Jr.; Peralta, J. E.; Ogliaro, F.; Bearpark, M.; Heyd, J. J.; Brothers, E.; Kudin, K. N.; Staroverov, V. N.; Kobayashi, R.; Normand, J.; Raghavachari, K.; Rendell, A.; Burant, J. C.; Iyengar, S. S.; Tomasi, J.; Cossi, M.; Rega, N.; Millam, N. J.; Klene, M.; Knox, J. E.; Cross, J. B.; Bakken, V.; Adamo, C.; Jaramillo, J.; Gomperts, R.; Stratmann, R. E.; Yazyev, O.; Austin, A. J.; Cammi, R.; Pomelli, C.; Ochterski, J. W.; Martin, R. L.; Morokuma, K.; Zakrzewski, V. G.; Voth, G. A.; Salvador, P.; Dannenberg, J. J.; Dapprich, S.; Daniels, A. D.; Farkas, Ö.; Foresman, J. B.; Ortiz, J. V.; Cioslowski, J.; Fox, D. J. *Gaussian 09*, revision A.01; Gaussian Inc.: Wallingford, CT, 2009.
(50) TURBOMOLE V6.3, a development of University of Karlsruhe and Forschungszentrum Karlsruhe GmbH, 1989−2007, TURBOMOLE GmbH, since 2007. Available from http://www.turbomole.com.
(51) Weigend, F. *J. Comput. Chem.* **2008**, *29*, 167−175.
(52) Weigend, F.; Häser, M.; Patzelt, H.; Ahlrichs, R. *Chem. Phys. Lett.* **1998**, *294*, 143−152.
(53) Hellweg, A.; Hättig, C.; Höfener, S.; Klopper, W. *Theor. Chem. Acc.* **2007**, *117*, 587−597.
(54) Weigend, F.; Ahlrichs, R. *Phys. Chem. Chem. Phys.* **2005**, *7*, 3297−3305.
(55) Peterson, K. A.; Puzzarini, C. *Theor. Chem. Acc.* **2005**, *114*, 283−296.
(56) Hampel, C.; Peterson, K. A.; Werner, H.-J. *Chem. Phys. Lett.* **1992**, *190*, 1−12.

(57) Deegan, M. J. O.; Knowles, P. J. *Chem. Phys. Lett.* **1994**, *227*, 321−326.
(58) Bartlett, R. J.; Musiał, M. *Rev. Mod. Phys.* **2007**, *79*, 291−352.
(59) Shavitt, I.; Bartlett, R. J. *Many-Body Methods in Chemistry and Physics*; Cambridge Molecular Science, Cambridge University Press: Cambridge, U. K., 2009.
(60) van Leeuwen, R.; van Lenthe, E.; Baerends, E. J.; Snijders, J. G. *J. Chem. Phys.* **1994**, *101*, 1272−1281.
(61) te Velde, G.; Bickelhaupt, F. M.; Baerends, E. J.; Fonseca Guerra, C.; van Gisbergen, S. J. A.; Snijders, J. G.; Ziegler, T. *J. Comput. Chem.* **2001**, *22*, 931−967.
(62) Fonseca Guerra, C.; Snijders, J. G.; te Velde, G.; Baerends, E. J. *Theor. Chem. Acc.* **1998**, *99*, 391−403.
(63) *ADF User's Guide*, Release 2010.1; SCM, Theoretical Chemistry, Vrije Universiteit: Amsterdam, The Netherlands, 2010. http://www.scm.com.
(64) Belpassi, L.; Storchi, L.; Quiney, H. M.; Tarantelli, F. *Phys. Chem. Chem. Phys.* **2011**, *13*, 12368−12394.
(65) Storchi, L.; Belpassi, L.; Tarantelli, F.; Sgamellotti, A.; Quiney, H. M. *J. Chem. Theory Comput.* **2010**, *6*, 384−394.
(66) Grant, I. P. *Relativistic Quantum Theory of Atoms And Molecules*, 1st ed.; Springer-Verlag: New York, 2006; Vol. *1*.
(67) Storchi, L.; Rampino, S.; Belpassi, L.; Tarantelli, F.; Quiney, H. M. *J. Chem. Theory Comput.* **2013**, *9*, 5356−5364.
(68) Dyall, K. G. *Theor. Chem. Acc.* **2007**, *117*, 483. Available from the Dirac web site: http://dirac.chem.sdu.dk.
(69) Dyall, K. G. *Theor. Chem. Acc.* **2012**, *131*, 1217. Available from the Dirac web site: http://dirac.chem.sdu.dk.
(70) Grant, I. P.; Quiney, H. M. *Phys. Rev. A* **2000**, *62*, 022508.
(71) Baenziger, N. C.; Dittemore, K. M.; Doyle, J. R. *Inorg. Chem.* **1974**, *13*, 805−811.
(72) Schwerdtfeger, P.; Hermann, H. L.; Schmidbaur, H. *Inorg. Chem.* **2003**, *42*, 1334−1342.
(73) Carvajal, M. A.; Novoa, J. J.; Alvarez, S. *J. Am. Chem. Soc.* **2004**, *126*, 1465−1477.
(74) Schmidbaur, H.; Shiotani, A.; Klein, H. F. *J. Am. Chem. Soc.* **1971**, *93*, 1555−1557.
(75) Brown, T. J.; Dickens, M. G.; Widenhoefer, R. A. *J. Am. Chem. Soc.* **2009**, *131*, 6350−6351.
(76) Isab, A. A.; Sadler, P. J. *J. Chem. Soc., Dalton Trans.* **1982**, 135−141.
(77) Kennedy-Smith, J. J.; Staben, S. T.; Toste, F. D. *J. Am. Chem. Soc.* **2004**, *126*, 4526−4527.
(78) Zhou, C.-Y.; Chan, P. W. H.; Che, C.-M. *Org. Lett.* **2006**, *8*, 325−328.
(79) Zuccaccia, D.; Belpassi, L.; Macchioni, A.; Tarantelli, F. *Eur. J. Inorg. Chem.* **2013**, *2013*, 4121−4135.
(80) Bistoni, G.; Belpassi, L.; Tarantelli, F. *Angew. Chem., Int. Ed.* **2013**, *52*, 11599−11602.
(81) Dias, H. V. R.; Flores, J. A.; Wu, J.; Kroll, P. *J. Am. Chem. Soc.* **2009**, *131*, 11249−11255.
(82) Karton, A.; Martin, J. *Theor. Chem. Acc.* **2006**, *115*, 330−333.
(83) Truhlar, D. G. *Chem. Phys. Lett.* **1998**, *294*, 45−48.
(84) Boys, S. F.; Bernardi, F. *Mol. Phys.* **1970**, *19*, 553−566.
(85) Mentel, L. M.; Baerends, E. J. *J. Chem. Theory Comput.* **2014**, *10*, 252−267.
(86) Pyykko, P. *Chem. Soc. Rev.* **2008**, *37*, 1967−1997.
(87) Belpassi, L.; Infante, I.; Tarantelli, F.; Visscher, L. *J. Am. Chem. Soc.* **2008**, *130*, 1048−1060.
(88) Kang, R. H.; Yao, J.; Chen, H. *J. Chem. Theory Comput.* **2013**, *9*, 1872−1879.
(89) Sun, Y. Y.; Chen, H. *J. Chem. Theory Comput.* **2013**, *9*, 4735−4743.
(90) Sun, Y.; Chen, H. *J. Chem. Theory Comput.* **2014**, Available ASAP, DOI: 10.1021/ct4010855.
(91) Grimme, S.; Antony, J.; Ehrlich, S.; Krieg, H. *J. Chem. Phys.* **2010**, *132*, 154104.